

# Investigation of Optically Controlled Millimeter Wave Coplanar Waveguide Photoconductive Device

J. SOBOLEWSKI<sup>a,\*</sup>, Y. YASHCHYSHYN<sup>a</sup>, D. VYNNYK<sup>b</sup>,  
V. HAIDUCHOK<sup>b</sup> AND N. ANDRUSHCHAK<sup>c</sup>

<sup>a</sup> *Warsaw University of Technology, Institute of Radioelectronics and Multimedia Technology, Nowowiejska 15/19, 00-665 Warsaw, Poland*

<sup>b</sup> *Scientific-Research Company "Electron — Carat", Stryiska 202, 79031 Lviv, Ukraine*

<sup>c</sup> *Lviv National Polytechnic University, S. Bandery 12, 79013 Lviv, Ukraine*

Doi: [10.12693/APhysPolA.141.420](https://doi.org/10.12693/APhysPolA.141.420)

\*e-mail: [j.sobolewski@ire.pw.edu.pl](mailto:j.sobolewski@ire.pw.edu.pl)

Devices based on photoconductive materials are promising solutions for future reconfigurable millimeter-wave communication systems. So far, there are several examples of photoconductive radio-frequency switches in the literature, however, their operating frequency and performance are low compared to other radio-frequency switching techniques. In this paper, we propose different photoconductive switch topologies based on the coplanar waveguide, which is more suitable for millimeter-wave applications than the published solutions. The utilization of germanium as the photoconductive element is also evaluated. The main advantages of germanium are its high carrier mobility and lifetime, which facilitates the creation of efficient devices, uniform carrier concentration in thick layers, which enhances interaction with the electromagnetic field in transmission line as well as sensitivity in 1.5  $\mu\text{m}$  spectral region, which simplifies the integration of radio-frequency equipment based on photoconductive devices with existing telecommunication networks. The construction of the switch was evaluated using full-wave electromagnetic simulations based on the finite-difference time-domain method. The influence of the photoconductive substrate conductivity changes on the transmission and reflection characteristics of the coplanar waveguide was investigated. Additionally, the feasibility of the utilization of thin-film photoconductive materials in the proposed switch was examined.

topics: photoconductivity, RF switching, reconfigurable devices, millimeter-wave

## 1. Introduction

One of the most important aspects of next-generation communication systems is their reconfigurability, which allows them to adapt to continuously changing conditions, such as the number of users, their movement and the type of propagation environment. This flexibility enables more efficient utilization of system resources, leading to lower power consumption and system costs, as well as better services performance. The key components of reconfigurable millimeter-wave (mm-wave) systems are radio-frequency (RF) switching devices.

As most of the currently used telecommunication backbone networks are based on optical systems, optically-controlled RF components are of great interest for the interface between wired and wireless parts of the networks. The application of optically-controlled RF components allows easier interfacing with optical networks and simplifies the construction of some reconfigurable devices.

Electrically-controlled components require routing of low-frequency signals and bias voltage in close proximity to mm-wave transmission lines, which is often challenging and leads to losses. In the case of optically-driven devices, the control signal can be applied from a distance and routed with non-conductive elements.

One of the concepts for optically-controlled RF devices is the utilization of photoconductivity phenomenon in semiconductors. It allows changing the electrical conductivity of the semiconductor by changing the intensity of light incident to its surface. Some examples of such devices can be found in the literature; however, this topic is still not thoroughly investigated. One of the applications for photoconductive materials is reconfigurable antennas [1–5]. A popular concept for reconfigurable antennas is a projection of light pattern on the semiconductor surface, which can be used for frequency tuning (by adjusting the size of antenna elements) [3] or for changing the radiation

pattern (by changing the location of antenna elements) [1, 2, 4, 5]. Other applications for photoconductive materials in RF devices are switches and variable attenuators [6–9]. These devices are more universal and can be used, for example, for switching between antenna elements, modification of antenna arrays, or switching between different signal paths in reconfigurable transmitters and receivers. However, these photoconductive material-based RF series switching devices exhibit poor performance, especially in the mm-wave region.

In this paper, we investigate the construction of a parallel topology photoconductive switching device based on a coplanar waveguide on the germanium substrate.

## 2. Photoconductive switch/modulator design

### 2.1. Photoconductive material

Most of the published optically-controlled RF devices are based on silicon. It is often used due to its relatively low intrinsic carrier concentration and, therefore, low intrinsic conductivity, moderate carrier mobility, and high carrier lifetime (Table I) [10, 11]. It is also an easily available and low-cost material, which makes it preferable to materials with better photoconductive properties. Also, as the optimal illumination wavelength for the effective operation of photoconductive devices depends on the bandgap of the material and its absorption characteristics, the silicon-based devices require a control signal wavelength around 0.8  $\mu\text{m}$ . Therefore they can be controlled even by instruments working in visible light range. In contrast, most telecommunication networks typically operate at higher wavelengths around 1.5  $\mu\text{m}$ , where optical fiber attenuation is lower.

In this paper, germanium was chosen due to its several advantages. First, it exhibits significantly higher carrier mobilities than silicon, higher carrier lifetime and absorption. These parameters determine carrier concentration in illuminated semiconductor and therefore its conductivity which can be derived from [12]

$$\sigma = \sigma_i + e\mu_n \Delta n + e\mu_p \Delta p, \quad (1)$$

where  $\sigma_i$  is the intrinsic semiconductor conductivity,  $e$  is the elementary charge,  $\mu_n$  and  $\mu_p$  are electron and hole mobilities, respectively, and  $\Delta n$  and  $\Delta p$  are photoinduced electron and hole concentrations in the semiconductor. Intrinsic semiconductor conductivity can be derived from

$$\sigma_i = e n_i (\mu_n + \mu_p), \quad (2)$$

where  $n_i$  is the intrinsic carrier concentration. The photo-induced carrier concentration can be derived from [12]

$$\frac{d^2 [\Delta n(u)]}{du^2} + \frac{\Delta n(u)}{L_a^2} + \frac{\tau g(u)}{L_a^2} = 0, \quad (3)$$

TABLE I

Optical and electrical properties of intrinsic semiconductor substrates [10, 11].

Parameters	Si	Ge
dielectric constant at 100 GHz	11.7	16
absorption coefficient at $\lambda = 550 \text{ nm}$ [ $\text{cm}^{-1}$ ]	$6.70 \times 10^3$	$5.03 \times 10^5$
intrinsic carrier concentration [ $\text{cm}^{-3}$ ]	$1.45 \times 10^{10}$	$2.40 \times 10^{13}$
electron mobility [ $\text{cm}^2/(\text{V s})$ ]	1500	3900
hole mobility [ $\text{cm}^2/(\text{V s})$ ]	450	1900
effective carrier lifetime [s]	$10^{-4}$	$10^{-3}$
diffusion coefficient [ $\text{cm}^2/\text{s}$ ]	17.31	63.88

where  $u$  indicates the coordinates,  $\tau$  is the carrier lifetime,  $g$  is the generation rate proportional to illumination power density, and  $L_a$  is the diffusion length. The drawback of the germanium compared to silicon is its higher intrinsic carrier concentration, leading to higher intrinsic conductivity (around 2.23 S/m).

The second important advantage of germanium is its higher efficiency than of silicon. As demonstrated in [13], to achieve a similar carrier concentration in the semiconductor sample, the optical power density can be almost two times lower for germanium than silicon.

Another important aspect, especially for transmission line-based switch or modulator, is the uniformity of carrier concentration profiles for high thickness germanium layers [13]. As the electromagnetic field in the transmission line penetrates quite deep into the dielectric substrate, the light-induced conductivity changes in the bulk of the material are required to effectively influence the transmission in the line.

Germanium photoconductive element also allows efficient operation in the 1.5  $\mu\text{m}$  spectral region, making it compatible with equipment widely used in telecommunication networks. As a result, optical driving circuits for a photoconductive device can use cost-effective and widely available mass-produced optical components. Moreover, it simplifies the interface between devices using photoconductive devices and external equipment. Considering the aforementioned characteristics, germanium is a good candidate to be used as an active element or devices for future telecommunication equipment.

### 2.2. Device construction

The construction of RF switches and variable attenuators using photoconductive materials found in the literature is mainly based on a microstrip transmission line (MSL) [7–9]. MSL consists of the signal conductor suspended on the dielectric layer above the ground plane. In such a line electromagnetic

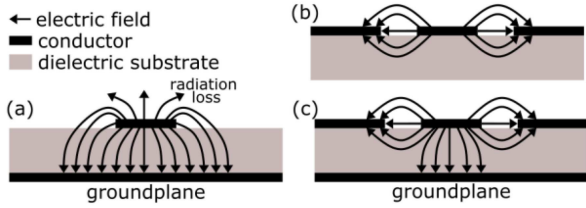


Fig. 1. Electric field distributions in the cross-section of (a) MSL, (b) CPW and (c) CPWG transmission lines.

field is concentrated in the substrate material directly below and in the close vicinity of the signal conductor and partially in the air (Fig. 1a). Therefore, the construction of such a line requires a relatively electrically (relative to wavelength) thin substrate. It also suffers from high radiation losses, especially with lower substrate permittivity. Another disadvantage of MSL, especially pronounced at high frequencies, is difficulty of maintaining signal integrity in connections between MSL and other components. MSL construction also determines the switching device topology as only series devices (where photoconductive material replaces a section of the signal conductor) are practically feasible. However, series switches are rarely used in high-frequency applications due to their poor performance.

The transmission line often used in mm-wave circuits is coplanar waveguide (CPW). This type of line consists of three conductors: a signal line in the center and two ground conductors on the sides. In such a line, the electromagnetic field is concentrated in the region between signal and ground conductor, partially in a substrate and partially in the air (Fig. 1b). It exhibits very low radiation losses and can be easily interfaced with other components such as integrated circuits or with test equipment (using RF probes). A special case of CPW is conductor-backed or grounded CPW (CPWG), where the opposite side of the CPW substrate is also used as a ground conductor. In CPWG, part of the electromagnetic field is concentrated between a central conductor and ground plane, similar to MSL. However, with high substrate thickness, field intensity between the center conductor and ground plane becomes very small, and the line can be regarded as CPW. As in CPW, the field is concentrated mostly in the region between conductors, it allows the construction of parallel/shunt topology switch where the substrate can be used as an active element. If the CPW is constructed on the photoconductive substrate, illumination from the top of the line influences conductivity of the exposed areas between conductors. With sufficiently high photo-induced conductivity, the illuminated region creates short-circuit in the CPW, therefore, working as a reflective SPST switch.

### 2.3. Simulation models

To evaluate the influence of substrate conductivity changes on the transmission of the RF signal in CPW, full-wave electromagnetic simulations utilizing the finite-difference time-domain (FDTD) method were carried out using CST Microwave Studio software. Three types of simulation models of CPW were created. The first model is a CPWG line section on a single layer, 100  $\mu\text{m}$  thick semiconductor substrate with permittivity  $\epsilon_r = 16$ , representing germanium (Fig. 2a). The second model is a CPWG line section on two-layer substrate (Fig. 2b). The top layer, directly under the signal conductor, is a 100  $\mu\text{m}$  thick layer of semiconductor with permittivity  $\epsilon_r = 16$ . Below it is a 1 mm thick dielectric layer with permittivity  $\epsilon_r = 9.4$  and loss tangent  $\tan(\delta) = 0.0004$ , representing alumina. The purpose of the dielectric layer is to provide mechanical support for the semiconductor layer, as the device with a single 100  $\mu\text{m}$  layer can be difficult to manufacture and impractical to use. The third model (Fig. 2c) is a CPWG line section on a single layer, 2 mm germanium semiconductor substrate. The length of all models is equal to 2.5 mm. All conductive surfaces are modeled as 0.7  $\mu\text{m}$  thick copper layer. The transmission line section in the models was terminated with 50  $\Omega$  impedance excitation ports on both ends to calculate the full scattering matrix.

### 3. Evaluation

To evaluate mm-wave and also microwave performance of photoconductive substrate-based CPWG, the simulations were carried out for a wide frequency range from 1 GHz to 300 GHz. As the simulation models are symmetrical, transmission and reflection coefficients obtained with excitation from both ports are identical. Therefore, only  $S_{21}$  and  $S_{11}$  elements of scattering matrices are presented.

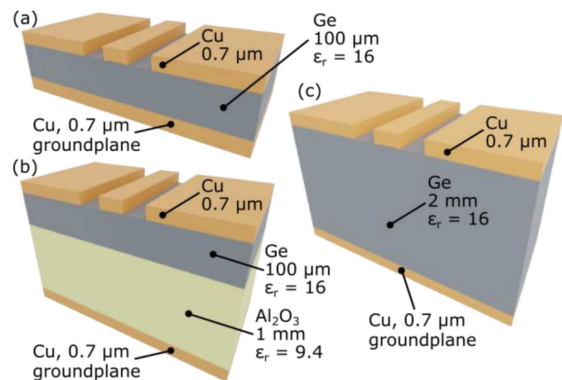


Fig. 2. (a) Single-layer thin semiconductor substrate simulation model cross-section. (b) Two-layer simulation model cross-section. (c) Single-layer thick semiconductor substrate simulation model cross-section.

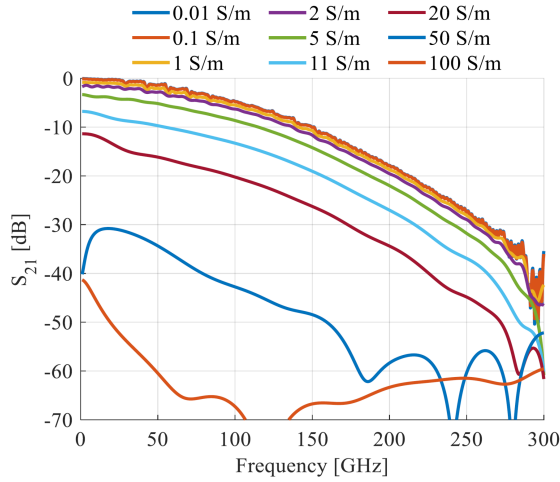


Fig. 3. Frequency characteristics of transmission coefficient ( $S_{21}$ ) in the section of the CPWG line on  $100 \mu\text{m}$  single layer substrate at different substrate conductivities.

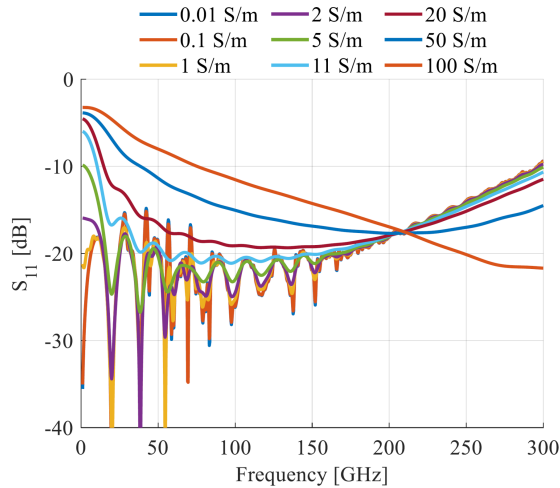


Fig. 4. Frequency characteristics of reflection coefficient ( $S_{11}$ ) in the section of the CPWG line on  $100 \mu\text{m}$  single layer substrate at different substrate conductivities.

In Fig. 3, characteristics of transmission coefficient for single-layer thin semiconductor substrate (Fig. 2a) are presented. As can be seen with substrate conductivity up to  $2 \text{ S/m}$ , the attenuation changes are very small. This indicates that the losses visible at higher frequencies can be contributed to lossy conductors. Thus, the losses introduced by the intrinsic germanium substrate in the off-state (without illumination) can be considered negligible.

Also, as shown in Fig. 4, the reflections in the line at these conductivity levels are also low up to about  $200 \text{ GHz}$ , indicating that line characteristic impedance is sufficiently maintained. Moderate reflection coefficient values and their increase above  $200 \text{ GHz}$  indicate some impedance mismatch

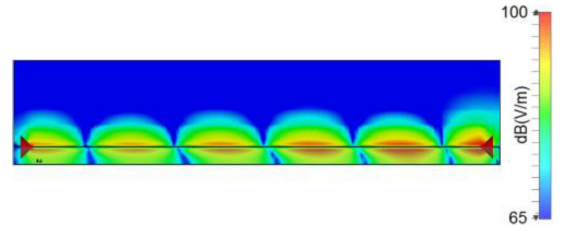


Fig. 5. Electric field distribution at the longitudinal section of CPWG line on  $100 \mu\text{m}$  single layer substrate.

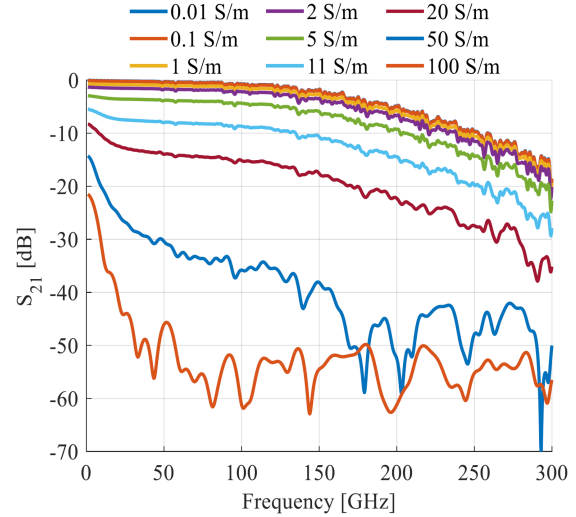


Fig. 6. Frequency characteristics of transmission coefficient ( $S_{21}$ ) in the section of CPWG line on two-layer substrate at different top layer conductivities.

between the transmission line and  $50 \Omega$  ports. It can be attributed to the influence of the field concentration (Fig. 5) between the central conductor and groundplane, shifting the line characteristic impedance.

On the other hand, with attenuation values over  $30 \text{ dB}$  (Fig. 3) in the whole considered frequency range achieved with substrate conductivity of  $50 \text{ S/m}$  the device can be regarded as an effective switch. Considering that conductivity of the illuminated germanium can achieve values order of magnitude higher (e.g.  $240 \text{ S/m}$  at  $200 \text{ mW/cm}^2$  [14],  $900 \text{ S/m}$  at  $1 \text{ W/cm}^2$  [13]), this type of switch can perform better than currently used conventional constructions based on transistors and PIN diodes. Quite a low reflection coefficient values at high substrate conductivity indicate that in on-state part of the energy is absorbed in the semiconductor, especially at higher frequencies resembling the behavior of the absorptive RF switch.

As the manufacturing and handling of the device using very thin semiconductor substrate can be problematic, the model with a semiconductor layer supported with dielectric was analyzed. In Fig. 6, transmission characteristics are calculated

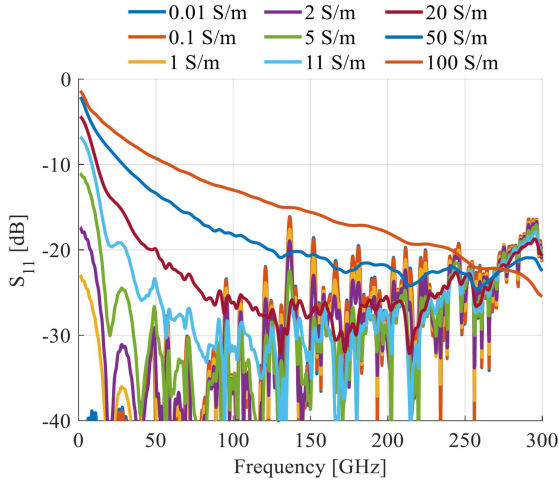


Fig. 7. Frequency characteristics of reflection coefficient ( $S_{11}$ ) in the section of CPWG line on two-layer substrate at different top layer conductivities.

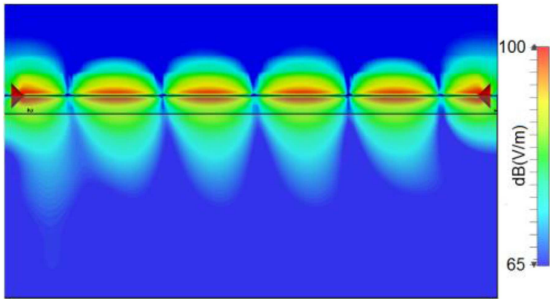


Fig. 8. Electric field distribution at the longitudinal section of CPWG line on two-layer substrate.

with two-layer model (Fig. 2b) with varying semiconductor layer conductivity. As can be seen, the sensitivity of the model to conductivity changes is noticeably smaller than for single-layer substrate despite the same semiconductor thickness. The differences are especially visible at frequencies over 100 GHz and at higher conductivity values. Furthermore, attenuation in the on-state (with illumination) is about 10 dB lower than for the structure with a single layer. It should also be noted that off-state attenuation is also considerably lower, especially above 100 GHz.

The reflection coefficient characteristics (Fig. 7) show better impedance matching to 50  $\Omega$  than single-layer thin substrate, as the influence of the ground plane diminishes.

It can be observed in Fig. 8 that the electric field is concentrated in the semiconductor layer and also penetrates the dielectric. However, with high substrate thickness, the field concentration region does not reach the ground plane.

The third analyzed case was the possibility to use a more robust, 2 mm thick single-layer semiconductor substrate (Fig. 2c) to simplify the device construction. The simulated transmission

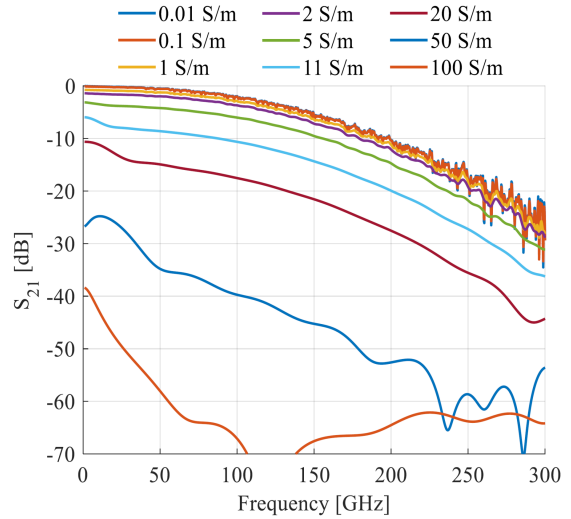


Fig. 9. Frequency characteristics of transmission coefficient ( $S_{21}$ ) in the section of CPWG line on 2 mm single layer substrate at different substrate conductivities.

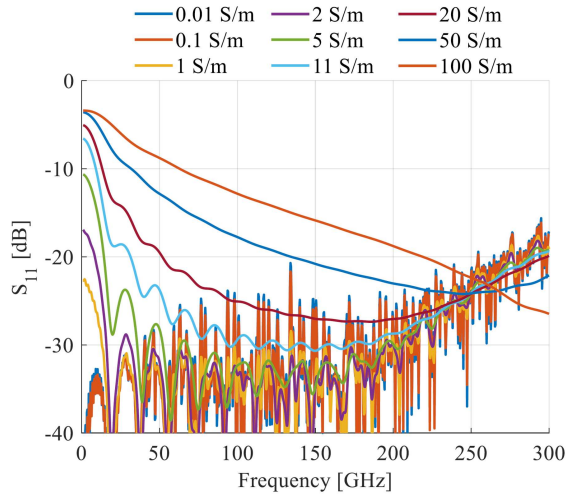


Fig. 10. Frequency characteristics of reflection coefficient ( $S_{11}$ ) in the section of CPWG line on 2 mm single layer substrate at different substrate conductivities.

characteristics for this model are shown in Fig. 9. In the off-state, with low substrate conductivity, the attenuation in the line is slightly higher than with two-layer substrates, but still noticeably lower than in the case of a thin single-layer semiconductor substrate. As a result, the sensitivity to the conductivity changes is considerably higher than for two-layer substrate and similar to a thin semiconductor substrate.

The reflection coefficient characteristics (Fig. 10) are very similar to those obtained for two-layer substrate with well impedance matching across a wide frequency range. As can be noted in the field distribution diagram shown in Fig. 11 there are higher modes excited in the semiconductor substrate due

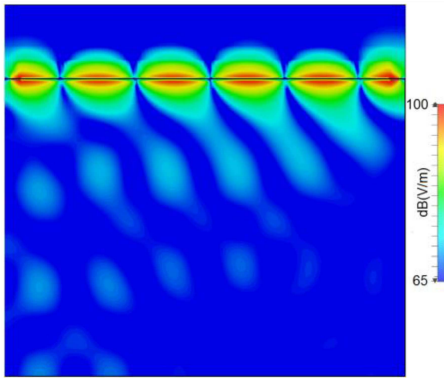


Fig. 11. Electric field distribution at the longitudinal section of CPWG line on 2 mm single layer substrate.

to its high permittivity and high thickness compared to the wavelength. These modes can contribute to increased attenuation visible in Fig. 9. The coupling for these modes from CPWG is weak, however, special consideration is needed for the integration of such devices to avoid the creation of high coupling at the feed point.

#### 4. Conclusions

The construction of the photoconductive RF switch for mm-wave frequency range based on coplanar waveguide was investigated. The proposed switch utilizes shunt topology often used in a transistor and PIN-diode-based RF switches contrary to other published photoconductive devices. It allows achieving better RF performance with low insertion loss in the off-state and high attenuation in the on-state. Moreover, the application of germanium as a photoconductive element was considered due to its better performance than silicon and suitability for operating with commonly available telecommunication equipment working in a  $1.5 \mu\text{m}$  spectral region. Performed electromagnetic simulations show that the proposed device offers good performance with more than 30 dB on-off ratio at conductivity changes between 2 S/m and 50 S/m which in the case of germanium does not require very high optical power.

Analysis of three different substrate arrangements shows that the highest on-state attenuation can be achieved with a thin single-layer semiconductor. However, this construction exhibits high off-state attenuation and can be impractical to manufacture and use due to its fragility. Application of an additional dielectric layer ensures more robust construction and decreases the off-state losses at the cost of inferior on-state performance and much more complicated manufacturing. A good compromise between on and off-state performance as well as robustness and straightforward manufacturing can be achieved using construction with the thick single-layer semiconductor substrate.

#### Acknowledgments

This work is part of a project IMAGE that has received funding from the European Union's Horizon2020 research and innovation programme under the Marie Skłodowska-Curie grant agreement No 778156.

#### References

- [1] M.I.B. Shams, Z. Jiang, J. Qayyum, S. Rahman, P. Fay, L. Liu, in: *2015 IEEE MTT-S Int. Microwave Symposium*, 2015, p. 1.
- [2] T.F. Gallacher, D.A. Robertson, G.M. Smith, *IEEE Trans. Antennas Propag.* **61**, 1688 (2013).
- [3] V. Sathi, N. Ehteshami, J. Nourinia, *IEEE Antennas Wireless Propag. Lett.* **11**, 1018 (2012).
- [4] T.F. Gallacher, R. Sondena, D.A. Robertson, G.M. Smith, *IEEE Trans. Microw. Theory Tech.* **60**, 2301 (2012).
- [5] I.F. da Costa, A.S. Cerqueira, D.H. Spadoti, L.G. da Silva, J.A.J. Ribeiro, S.E. Barbin, *IEEE Antennas Wireless Propag. Lett.* **16**, 2142 (2017).
- [6] P. Alizadeh, A.S. Andy, C. Parini, K.Z. Rajab, in: *10th European Conf. on Antennas and Propagation (EuCAP)*, 2016, p. 1.
- [7] H. Su, I. Shoaib, X. Chen, T. Kreouzis, in: *IEEE Asia-Pacific Conf. on Antennas and Propagation*, 2012, p. 265.
- [8] S. Pendharker, R.K. Shevgaonkar, A.N. Chandorkar, *IEEE Antennas Wireless Propag. Lett.* **13**, 99 (2014).
- [9] Y. Tawk, A.R. Albrecht, S. Hemmady, G. Balakrishnan, C.G. Christodoulou, *IEEE Antennas Wireless Propag. Lett.* **9**, 280 (2010).
- [10] E.D. Palik, *Handbook of Optical Constants of Solids*, Academic Press 1998.
- [11] S.M. Sze, K.K. Ng, *Physics of Semiconductor Devices*, John Wiley & Sons 2006.
- [12] R.B. Adler, A.C. Smith, R.L. Longini, *Introduction to Semiconductor Physics*, Wiley, New York 1964.
- [13] A. Kannegulla, Md.I. Bin Shams, L. Liu, L. Cheng, *Opt. Express* **23**, 32098 (2015).
- [14] R. Cane, R. Sauleau, M. Alouini, in: *49th European Microwave Conf. (EuMC)*, 2019, p. 714.